ELSEVIER

Journal of Power Sources 70 (1998) 34–39

JOURNAL OF POWER SOURCES

Lithium transport through graphite electrodes that contain two stage phases

Su-Il Pyun *, Young-Gyoon Ryu

Department of Materials Science and Engineering, Korea Advanced Institute of Science and Technology, 373-1 Kusong-Dong, Yusong-Gu 305-701, Daejon, South Korea

Received 20 November 1996; revised 27 February 1997

Abstract

The lithium transport through graphite electrodes that contain two stage phases has been investigated in 1 M $LiAsF_6$–EC/DEC (ethylene carbonate/diethyl carbonate) non-aqueous solution by using potentiostatic current transient technique supplemented by lithium charging/discharging experiments and a.c. impedance spectroscopy. An attractive interaction between the intercalated lithium ions and the graphite lattice is indicated from the decreased diffusivity value with increasing lithium content in the lithiated graphite electrode in the presence of a single stage phase. This attractive interaction gives rise to the stage transformation in the electrode, which is characterized by potential plateaus in the charge/discharge curves. From the results of the potentiostatic current transients, it is suggested that the stage transformation in the lithiated graphite electrode is accompanied by the limited transport of lithium through the electrode for which the stress generated by the stage phase boundary is responsible. The stress-controlled transport of lithium through the graphite structure is substantiated by the occurrence of hysteresis in the potential profile during the lithium intercalation and de-intercalation.

Keywords: Intercalation; Electrodes; Lithium; Diffusion; Stage transformation; Stage phase boundary

1. Introduction

Lithiated carbon ($Li_\delta C_6$) is used as a lithium-ion battery anode material; it shows good safety and excellent lithium charging/discharging cycleability in comparison with anodes made from lithium metal. Nevertheless, there are still some problems with respect to the destruction of the carbon structure (exfoliation) during lithium intercalation and the resulting decrease in specific energy. In order to inhibit the exfoliation of the carbon and to increase the specific energy of the lithiated carbon, many research efforts have focused on the electrochemical properties of the lithiated carbon electrode [1–3]. Ein-Eli et al. [3] reported that performance of electrodes containing lithiated carbon in rechargeable batteries is strongly dependent on the surface chemistry. On the other hand, Dahn et al. [4] studied the dependence of the electrochemical intercalation of the lithium into the lithiated carbon on the crystal structure of the carbon. It was found that highly graphitized carbons with flat voltage curves near 0.1 V_{Li/Li^+} and carbons with a large (002) half-width and a large strained region exhibit a high lithium capacity.

Another aspect of crucial importance in determining the performance of intercalation electrodes is related to the lithium transport through the lithiated host structure since this is the rate-determining step of the lithium intercalation process [5]. Generally, the kinetics of lithium transport through the layered structure is described in terms of concentration gradient, i.e., in terms of the rate of diffusion of lithium ions in the graphite electrode [5]. It should be realized, however, that a further determinant of the kinetics of the lithium transport through the graphite structure is the chemical potential gradient since the intercalation of lithium into graphite usually proceeds via a 'stage transformation' [6]. It is proposed that a phase boundary with large strain may exist between the two stage phases and its mobility determines the kinetics of the lithium intercalation into the graphite structure. Therefore, it is necessary to establish the lithium intercalation into the graphite structure during the coexistence of the two stage phases by using the appropriate electrochemical techniques.

* Corresponding author. Tel.: +82-42-869 33 02-4; Fax: +82-42-869 33 10.

0378-7753/98/$19.00
PII S0378-7753(97)02616-5

The present work aims to investigate lithium transport through graphite electrodes that contain two stage phases in equilibrium with each other. For this purpose, current-decay transients (chronoamperograms), charge/discharge curves and a.c. impedance spectra are measured on a lithiated graphite powder electrode in 1 M $LiAsF_6$–EC/DEC (ethylene carbonate/diethyl carbonate) solution at room temperature. The factors that affect lithium transport through lithiated graphite electrode with two stage phases are discussed in terms of interaction between the intercalated lithium and the stress field generated by the stage phase boundary.

2. Experimental

All electrochemical experiments were conducted in an argon-filled glove box (VAC HE493) at room temperature by using a three-electrode electrochemical cell. The working electrode was a PVDF (polyvinylidene fluoride)-bonded porous graphite electrode made from graphite powder (surface area: 9.8 $m^2\ g^{-1}$, Lonza KS-44). The porous graphite electrode specimen was manufactured by mixing the graphite powder with 10 wt.% PVDF as a binder, followed by pasting on a stainless-steel screen and drying in vacuum at 120 °C. Pure, lithium-metal foil was used for both the reference and counter electrodes. The lithium salt was 1 M $LiAsF_6$ and the solvent comprised a mixture of 50 vol.% EC and 50 vol.% DEC.

Lithium charge/discharge curves were measured by using a computerized multi-channel battery charger (Toyo system HRC 6064A). Galvanostatic charging and discharging currents corresponded to a change of $\delta = 1$ in $Li_\delta C_6$ in 10 h.

The a.c. impedance measurements were performed with a Solartron 1255 frequency response analyzer combined with Solartron 1286 electrochemical interface on the lithiated graphite powder electrode in 1 M $LiAsF_6$–EC/DEC solution at various electrode potentials of 0.05, 0.1, 0.15 and 0.25 versus V_{Li/Li^+}. An alternating sinusoidal signal of 10 mV peak-to-peak was superimposed on the d.c. potential. The impedance spectra were obtained over a frequency range of 1 mHz to 1 MHz.

Potentiostatic current transients were measured by using a potentiostat/galvanostat (EG&G PAR, Model 263). The graphite electrode was subjected to the initial applied potentials (0.1 to 0.16 V_{Li/Li^+}) for 10^4 s, followed a potential step to 0.01 V_{Li/Li^+}. At this stage, the resulting cathodic current was recorded versus time for 10^4 s (potentiostatic cathodic current transients). After measuring the cathodic current decay transient, the electrode potential was stepped from 0.01 V_{Li/Li^+} to the initial value. At this point, the resulting anodic current was recorded against time for 10^4 s (potentiostatic anodic current transients).

3. Results and discussion

3.1. Coexistence of two stage phases from charge-discharge curve

Fig. 1 shows the electrode potential, $E(\delta)$, as a function of time for a Lonza KS-44 graphite electrode charged and discharged using a constant current of 37.22 mA g^{-1} corresponds to a change $\Delta\delta = 1$ in $Li_\delta C_6$ in 10 h. Four potential plateaus near 0.07, 0.1, 0.2 and 1.0 V_{Li/Li^+} are observed during the first charge. The potential plateau near 1.0 V_{Li/Li^+} during the first charge disappeared in subsequent charges. There is a significant hysteresis in the potential profile during the intercalation (charging) and de-intercalation (discharging) of the lithium ions.

Potential plateaus in charge/discharge curves are usually found when the intercalation compound is comprised of coexisting phases over some range of lithium content, δ, in the graphite electrode [7]. There are many regions where phases with different stage indices coexist in the Li–C phase diagram [8]. According to a previous report [8], the potential plateaus are indexed as shown in Fig. 2. As the value of δ increases, transitions occur sequentially from a dilute stage-1 phase (denoted by 1′) through a stage-4, a liquid-like stage-2 phase (denoted by 2L), a stage-2 phase, and finally to a filled stage-1 phase. The sloping lines between the plateaus in Fig. 2 indicate the existence of only a single stage phase.

The disappearance of the potential plateau near 1.0 V_{Li/Li^+} after the first charge indicates the irreversible decomposition of electrolyte to form a passivating surface film on the lithiated graphite electrode [1,3,9,10]. It has

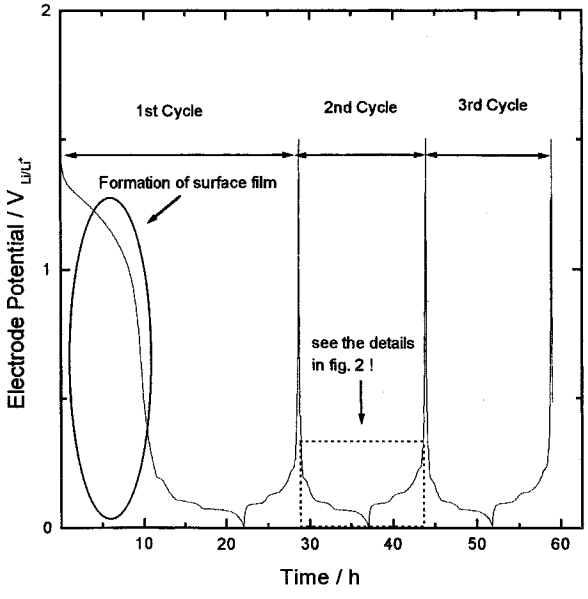

Fig. 1. Charge/discharge curve for a lithiated Lonza KS-44 graphite powder electrode in 1 M $LiAsF_6$–EC/DEC solution. Lithium charging and discharging currents correspond to a change $\Delta\delta = 1$ in $Li_\delta C_6$ in 10 h.

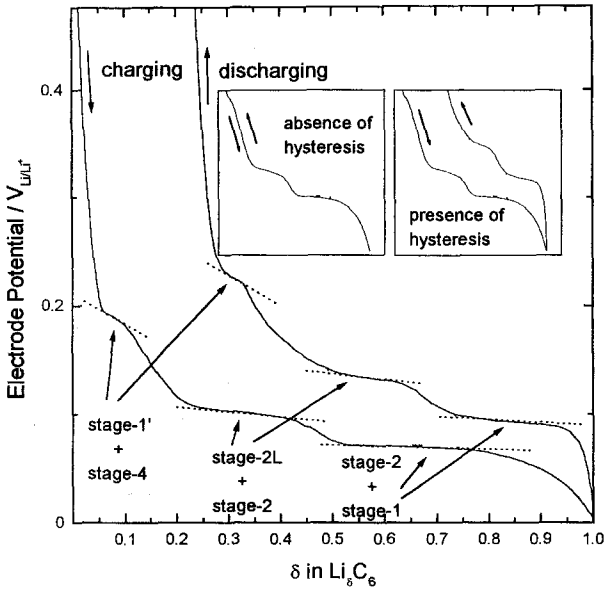

Fig. 2. Charge/discharge curve of a lithiated Lonza KS-44 graphite powder electrode in 1 M $LiAsF_6$–EC/DEC solution. Lithium charging and discharging currents correspond to a change $\Delta\delta = 1$ in $Li_\delta C_6$ in 10 h. The coexistence of two stage-phases is indexed in figure.

been reported that the energies associated with the coherency stresses required to hold together the phases of different lattice parameters may give rise to the hysteresis that is observed in the charge/discharge curves of the Li–C system [11]. Thus, it is concluded that occurrence of the hysteresis is due to the stress generated by the stage phase boundary.

3.2. Transport of lithium through the lithiated graphite in a single stage phase by a.c. impedance spectra

The a.c. impedance spectra obtained from a Lonza KS-44 graphite powder electrode in 1 M $LiAsF_6$–EC/DEC solution at 0.05, 0.08, 0.15, 0.25 V_{Li/Li^+} are presented in Fig. 3. At these potentials, only a single stage phase exists in the electrode. This is simply manifested by a sloping line in the charge/discharge curve, as shown in Fig. 2.

The impedance spectra consist of two depressed arcs in the high and middle frequency ranges, a line inclined at a constant angle of 45° to the real axis in the low-frequency range, and a capacitive line due to the accumulation of lithium at the center of the graphite particle in the frequency range below 10 mHz. The size of the high frequency arc is virtually unchanged with electrode potential. By contrast, the size of the middle frequency arc increases with increasing electrode potential.

In general, the surface film is found to be irreversibly formed and is stable in 1 M $LiAsF_6$–EC/DEC on the graphite surface near 1.0 V_{Li^+/Li^+} [1,3,9,10]. Thus, it is to be expected that the size of the arc is unaffected by the electrode potential. In this regard, the high-frequency arc appears to be due to the surface film formed on the lithiated graphite electrode. The charge-transfer resistance is associated with the middle-frequency arc and increases with increasing electrode potential due to the increased driving force for the lithium intercalation into the electrode. The inclined and capacitive lines in the low-frequency range are attributable to the Warburg impedance that is associated with the diffusion of lithium ions through the lithiated graphite electrode and the accumulation of lithium at the centre of the graphite particle, respectively.

It is very difficult to obtain a value for the diffusivity of lithium ions in the presence of the two stage phases since the movement of the stage phase boundary also contributes to the lithium transport through the graphite electrode and, thereby, results in a non-linear influence on the current response or potential response during the a.c. impedance measurements [12]. On the other hand, galvanostatic and potentiostatic intermittent titration techniques (GITT and PITT) have been used to obtain the diffusivity value of guest atoms such as lithium in the host lattice by many researchers [5,13]. In these techniques, derived mathematical expressions are based upon the rate-determining step of diffusion of the guest atoms through the host lattice. The rate-determining step of the lithium transport through lithiated graphite electrodes that contain two stage phases appears to be the movement of the phase boundary rather than the diffusion of lithium ions through the electrode. For this reason, the GITT and PITT are inappropriate to determine the diffusivity values of lithium ions in a lithiated graphite electrode that contains two stage phases.

In the present work, the chemical diffusivity of the lithium ion $\tilde{D}_{Li^+}$ in the graphite electrode in the presence of only a single stage phase is determined by analyzing the measured impedance spectra. The value of the chemical

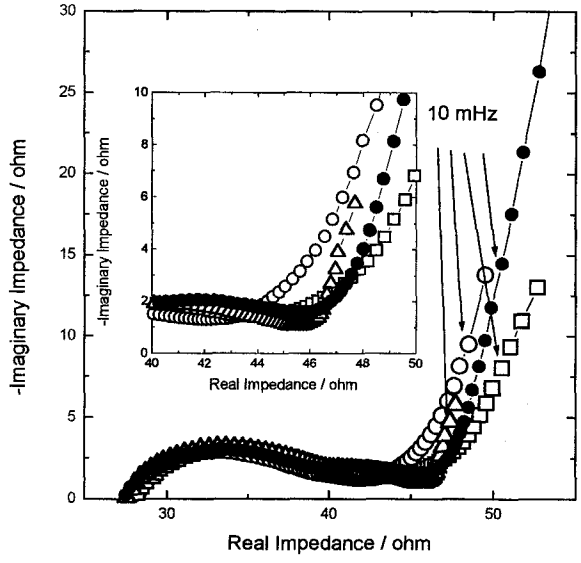

Fig. 3. A.c. impedance spectra obtained from a lithiated Lonza KS-44 graphite powder electrode in 1 M $LiAsF_6$–EC/DEC solution at (○) 0.05 V_{Li/Li^+}; (□) 0.08 V_{Li/Li^+}; (△) 0.15 V_{Li/Li^+}, V_{Li/Li^+} and (●) 0.25 V_{Li/Li^+}; in 1 M $LiAsF_6$–EC/DEC solution.

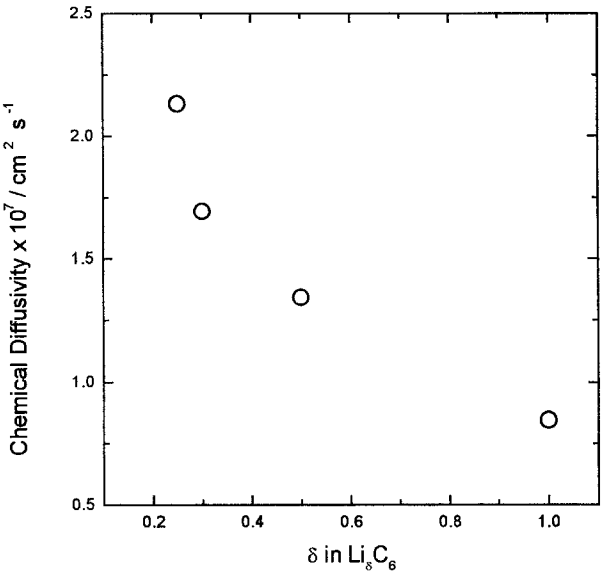

Fig. 4. Calculated chemical diffusivity $\tilde{D}_{Li^+}$ of lithium ions in a Lonza KS-44 graphite powder electrode as a function of lithium content.

diffusivity $\tilde{D}_{Li^+}$ is obtained by using Eq. (1) from the measured f_T and r values [14]

$$\tilde{D}_{Li^+} = \frac{\pi f_T r^2}{1.94} \quad (1)$$

where f_T is the frequency at which the impedance spectrum shows a transition from semi-infinite to finite-length diffusion behaviour, and r is the average radius of the Lonza KS-44 graphite powder, namely, 22 μm. The calculated $\tilde{D}_{Li^+}$ value of lithium ions is plotted versus the lithium content in the electrode in Fig. 4. The data show that the $\tilde{D}_{Li^+}$ value decreases with increasing lithium content. This indicates that there is attractive interaction between the intercalated lithium ions and the graphite lattice. This interaction gives rise to ordering of the intercalated lithium ions, i.e., a stage transformation, within the electrode. This result is substantiated by the occurrence of the potential plateaus in the charge/discharge curves.

3.3. Stress-controlled transport of lithium ions through lithiated graphite

In order to investigate the lithium transport through a lithiated graphite lattice with two stage phases, potentiostatic current transients were obtained for a Lonza KS-44 graphite powder electrode in 1 M $LiAsF_6$–EC/DEC solution. The potentiostatic cathodic and anodic current transients (on a logarithm–logarithm scale) are given in Figs. 5 and 6, respectively.

The current transients show two-step behaviour for both lithium intercalation (potential falling) and de-intercalation (potential rising). Irrespective of the applied electrode potential, the slopes of the initial step in the cathodic and anodic current transients are about −0.1 and −0.52, respectively. The anodic and cathodic currents decrease abruptly with time in the later step.

Assuming that the kinetics of the lithium transport during the lithium intercalation and de-intercalation is determined by the diffusion of lithium ions through the

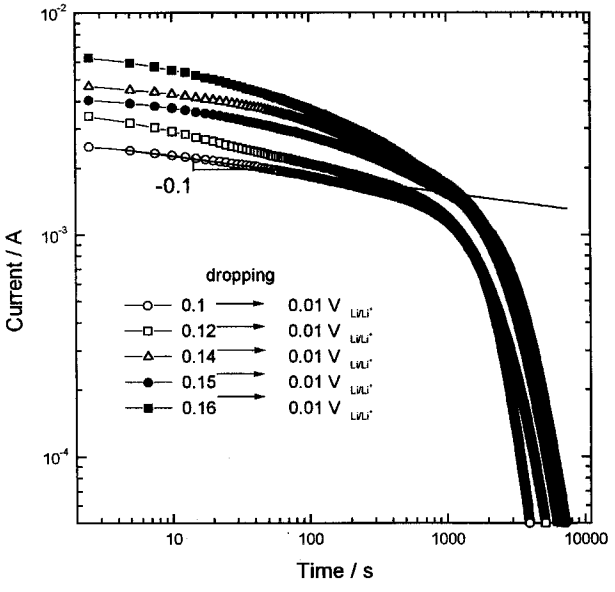

Fig. 5. Potentiostatic cathodic current transients for a lithiated graphite powder electrode obtained just after stepping down the electrode potential from (○) 0.1 V_{Li/Li^+}, (□) 0.12V_{Li/Li^+}, (△) 0.14 V_{Li/Li^+}, (●) 0.15 V_{Li/Li^+}, (■) 0.16 to 0.01 V_{Li/Li^+}, in 1 M $LiAsF_6$–EC/DEC solution.

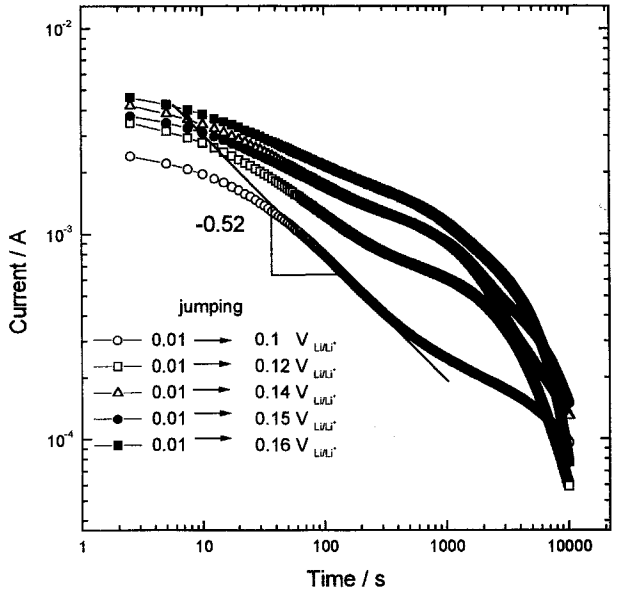

Fig. 6. Potentiostatic anodic current transients of a lithiated Lonza KS-44 graphite powder electrode obtained just after stepping up the electrode potential from 0.01 V_{Li/Li^+} to (○) 0.1 V_{Li/Li^+}, (□) 0.12 V_{Li/Li^+}, (△) 0.14 V_{Li/Li^+}, (●) 0.15 V_{Li/Li^+}, (■) 0.16 V_{Li/Li^+} in 1 M $LiAsF_6$–EC/DEC solution.

outer stage phase, then the resulting current transients can be expressed by Eq. (2) in the initial step and Eq. (3) in the later step [13]

$$I(t) = \frac{Q\sqrt{\tilde{D}_{Li^+}}}{l\sqrt{\pi}} t^{-\frac{1}{2}}, \quad t \ll \frac{l^2}{\tilde{D}_{Li^+}} \tag{2}$$

$$I(t) = \frac{2Q\tilde{D}_{Li^+}}{l^2} \exp\left(-\frac{\pi^2 \tilde{D}_{Li^+}}{4l^2} t\right), \quad t \gg \frac{l^2}{\tilde{D}_{Li^+}} \tag{3}$$

where $I(t)$ is the current as a function of time; Q is the total charge transferred during lithium intercalation; t is time; l is the thickness of the electrode with planar symmetry. In the present work, the thickness, l, of the outer stage phase is set at the equivalent $r/3$ for the radius r of the spherical graphite particle. According to Eq. (2), the slope of the initial step is -0.5 under diffusion control. The latter step is associated with the accummulation of lithium at the centre of the graphite electrode during lithium intercalation and the depletion of lithium in the graphite electrode during lithium de-intercalation.

Given the time-dependence of the current in the initial step (Eqs. (2) and (3)), it is inferred that another factor rather than the concentration gradient should affect the lithium transport through a lithiated graphite electrode in the presence of two stage phases. This is examined in the following discussion.

An intercalated lithium atom displaces the host atoms and sets up a strain field in the host lattice [11]. Since this strain field affects the energy of a second intercalated atom, this leads to an elastic interaction between the two intercalated atoms. In general, the graphite lattice is expanded by the lithium intercalation and this expansion imposes an energy penalty, which can be minimized by the phenomenon of 'staging' [6]. In addition, another strain field originates during the stage transformation since there exists a lattice-mismatched region between the stage phases, i.e., a stage phase boundary, which is already suggested by the hysteresis in potential profile of the charge/discharge curve, as shown in Fig. 2.

In the present work, the different slopes of the initial step current transients during the lithium intercalation and de-intercalation appear to be due to the stress field produced by the stage phase boundary rather than interaction between the intercalated lithium atoms. This is because the stress field associated with elastic interaction between intercalated atoms cannot give rise to the difference in the lithium transport behaviour during lithium intercalation and de-intercalation.

The coexistence of stage-1 and stage-2 phases is schematically illustrated in Fig. 7. When the stage-2 phase transforms into the stage-1 phase, the coexistence of stage-1 and stage-2 phases of the lithiated graphite can be envisaged by sandwiching an extra half plane of lithium atoms

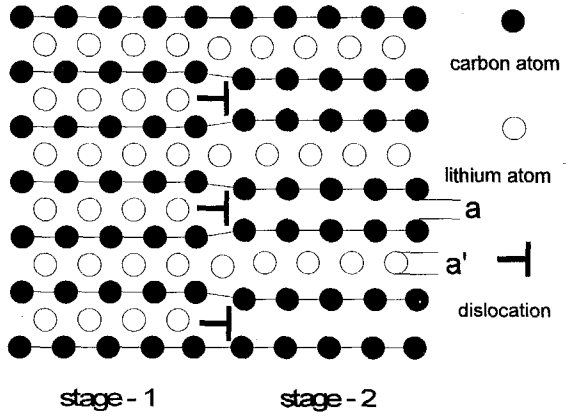

Fig. 7. Schematic illustration of the phase boundary between stage-1 and stage-2 phases in lithiated graphite.

between two graphite planes in stage-2 phase as host lattice. It seems that the intercalated lithium is arranged in the same way as the extra half plane of dislocation in the metal. It should be noted that whenever lithium intercalates or de-intercalates, a lithium-rich phase forms on the solution side of the graphite electrode because the characteristic array of lithium ions inside the graphite structure during the stage transformation, as shown in Fig. 7.

Considering dislocation mechanics [15], the point defect, i.e. intercalated lithium atom, and dislocations will interact elastically and exert forces on each other. To a good approximation, the strains around the point defect distort the lattice spherically, just as though an elastic sphere of radius a' had been forced into a spherical hole with a radius a in an elastic continuum. The resulting strain is $\epsilon = (a' - a)/a$. Considering the volume change produced by intercalated lithium atom and the hydrostatic component of the dislocation stress field, the interaction energy U_{int} between a intercalated lithium atom and a dislocation is given by

$$U_{int} = \frac{4(1+\nu)Gba^3\epsilon \sin\theta}{3(1-\nu)s} \tag{4}$$

where ν is the Poisson's ratio of graphite: G is the modulus of elasticity in shear: b is the Burgers vector: θ is the angle between the straight line from the dislocation core to the intercalated lithium atom and the Burgers vector; s represents the distance between the dislocation core and the intercalated lithium atom.

A negative value of the interaction energy indicates attraction between the intercalated lithium atom and the dislocation, while a positive value denotes repulsion. The intercalated lithium atom ($\epsilon > 1$) will be repelled from the compression side of a positive edge dislocation ($0 < \theta < \pi$). In this regard, it is clear that the strain field exerted by the stage phase boundary contributes to the chemical potential of the lithium ion in the graphite structure.

In general, the chemical potential, μ_{Li^+}, of lithium ions in a electrode material under a strain is expressed [16] as

$$\mu_{Li^+} = \mu^0_{Li^+} + U_{int} \quad (5)$$

where $\mu^0_{Li^+}$ is the chemical potential of lithium ions in the strain-free phase. Thus, the gradient in the chemical potential can be written as

$$\left(\frac{\partial \mu_{Li^+}}{\partial x}\right) = \left(\frac{\partial \mu^0_{Li^+}}{\partial x}\right) + \left(\frac{\partial U_{int}}{\partial x}\right) \quad (6)$$

and the flux of lithium atoms J, is

$$J = -cM_{Li^+}\left(\frac{\partial \mu_{Li^+}}{\partial x}\right) = -M_{Li^+}RT\left(\frac{\partial c}{\partial x}\right) - cM_{Li^+}\left(\frac{\partial U_{int}}{\partial x}\right) = -D_{Li^+}\left(\frac{\partial c}{\partial x}\right) - \frac{D_{Li^+}c}{RT}\left(\frac{\partial U_{int}}{\partial x}\right) \quad (7)$$

where c is the concentration of lithium in the graphite electrode; M_{Li^+} is the mobility of intercalated lithium ions in the graphite electrode under the stress field; R is the gas constant; T is the absolute temperature; D_{Li^+} is the diffusivity of lithium ions under the stress field. The first term in the right side of Eq. (7) corresponds to the contribution of the concentration gradient to the lithium-ion diffusion, while the second term represents the contribution of the strain energy gradient due to the lattice mismatch around the stage phase boundary. Therefore, the lithium-ion diffusion will be (i) retarded by the repulsive stress exerted by the stage phase boundary during lithium intercalation(stage-2 to stage-1 transformation), and (ii) enhanced during lithium de-intercalation (stage-1 to stage-2 transformation).

Considering that the initial slope of the current transient during lithium de-intercalation is steeper than that during lithium intercalation, it is suggested that the stress generated by the extra lithium plane retards and enhances the lithium transport through the lithiated graphite electrode during the lithium intercalation and de-intercalation, respectively.

4. Conclusions

The lithium transport through the graphite electrode was investigated in the presence of two stage phases by using a potentiostatic current transient technique complementarily with charge/discharge experiments and a.c. impedance spectroscopy. The following conclusions are drawn:

1. Given the occurrence of potential plateaus in the charge/discharge curve combined with the dependence of the chemical diffusivity of the lithium ion on lithium content in the lithiated graphite electrode, it is concluded that an attractive interaction between the intercalated lithium ion and the graphite lattice can account for the stage transformation of the electrode.
2. The stress generated around the stage phase boundary can be demonstrated by dislocation mechanics. The coexistence of stage-1 and stage-2 phases in the lithiated graphite can be realized by inserting extra lithium planes of lithium atoms into stage-2 as host lattice. From the potentiostatic current transient, it is inferred that the stress generated by the extra lithium plane retards and enhances the lithium transport through the lithiated graphite electrode during the lithium intercalation and de-intercalation, respectively. The stress-limited transport and stress-assisted transport of lithium through the lithiated graphite structure is confirmed by the occurrence of hysteresis in the potential profile during the lithium intercalation and de-intercalation, respectively.

Acknowledgements

This work was supported in 1996 by the Korea Science and Engineering Foundation through the Center for Interface Science and Engineering of Materials.

References

[1] J.O. Besenhard, M.W. Wagner and M. Winter, *J. Power Sources, 43–44* (1993) 413–420.
[2] S. Passerini, J.M. Rosolen and B. Scrosati, *J. Power Sources, 45* (1993) 333–341.
[3] Y. Ein-Eli, B. Markovsky, D. Aurbach, Y. Carmeli, H. Yamin and S. Luski, *Electrochim. Acta, 39* (1994) 2559–2569.
[4] J.R. Dahn, A.K. Sleigh, Hang Shi, J.N. Reimers, Q. Zhong and B.M. Way, *Electrochim. Acta, 38* (1993) 1179–1191.
[5] D. Guyomard and J. Tarascon, *J. Electrochem. Soc., 139* (1992) 937–948.
[6] M.S. Whittingham and A.J. Jacobson, *Intercalation Chemistry*, Academic Press, New York, 1982, p. 2.
[7] M.B. Armand, *Materials for Advanced Batteries*, Plenum, New York, 1980 p. 145–161.
[8] J.R. Dahn, *Phys. Rev. B, 44* (1991) 9170–9177.
[9] W. Ebner, D. Fouchard and L. Xie, *Solid State Ionics, 69* (1994) 238–256.
[10] Y.-G. Ryu and S.-I. Pyun, *J. Electroanal. Chem.*, (1997) accepted for publication.
[11] W.R. McKinnon and R.R. Haering, *Mod. Asp. Electrochem., 15* (1983) 274–280.
[12] A. Metro and A. Harrach, *Electrochim. Acta, 38* (1993) 2005–2009.
[13] C.J. Wen, B.A. Boukamp, R.A. Huggins and W. Weppner, *J. Electrochem. Soc., 126* (1979) 2258–2266.
[14] R. Cabanel, G. Barral, J.P. Diard, B. Le Gorrec and C. Montella, *J. Appl. Electrochem., 23* (1993) 93–97.
[15] G.E. Dieter, *Mechanical Metallurgy*, Mrated by the extra lithium plane179–180.
[16] R.A. Oriani, Invited Paper at *Symp. Chemical Effects of Elastic Stress, Spring Meet AIME, Boston, MA, USA, 1972.*